Hindawi
International Journal of Aerospace Engineering
Volume 2023, Article ID 8107966, 12 pages
https://doi.org/10.1155/2023/8107966

Research Article

Strain Prediction of Grain in Solid Rocket Motor under the Pressure Curing Molding Technology

Kaining Zhang[1], **Chunguang Wang**[1,2], **Qun Li**[1] and **Zhenyu Guo**[3]

[1]*State Key Laboratory for Strength and Vibration of Mechanical Structures, School of Aerospace Engineering, Xi'an Jiaotong University, Xi'an 710049, China*
[2]*Lingkong Tianxing Technology Co., Ltd., Beijing 100176, China*
[3]*Academy of Aerospace Solid Propulsion Technology, Xi'an 710025, China*

Correspondence should be addressed to Chunguang Wang; wangchunguang@xjtu.edu.cn

Received 27 August 2023; Revised 14 November 2023; Accepted 11 December 2023; Published 23 December 2023

Academic Editor: Vijayanandh Raja

The residual strain generated in grains during the propellant manufacturing process can significantly impact the safety and stability of solid rocket motors. Pressure curing molding technology has been employed as an effective approach to mitigate residual strain. This research paper focuses on deriving a strain prediction function for grains based on continuum mechanics, taking into account the influence of pressure curing molding technology. The accuracy of the prediction function is verified through finite element analysis. The results show that the proposed function accurately predicts strain distribution at critical positions within the grains. And the effects of curing pressure and the elastic modulus of the case on residual strain are analysed. Specifically, for a given material of case, an optimal curing pressure is identified that minimizes residual strain in the grains. Moreover, it is observed that materials with lower hoop elastic modulus, such as composites, tend to require lower optimal curing pressures. The outcomes of this study provide valuable guidance for grain shape design and the selection of optimal curing pressure.

1. Introduction

Solid rocket motors (SRMs) are widely used in space vehicles and spacecraft due to their simple structure, high reliability, and low cost. The grain serves as the power source of the SRM and is subjected to various loads from production to the launch process, resulting in stress and strain [1].

Currently, casting molding technology is widely used in the manufacturing process of grains. The propellant slurry solidifies into a propellant grain during the process of cooling from production temperature to room temperature under atmospheric conditions [2]. However, during the cooling process, the difference in thermal expansion coefficient between the grain and the case results in residual strain, which must be avoided as much as possible [3]. During the entire life cycle of a SRM, grains may undergo significant strains due to various loads, including temperature, gravity, and pressure. The accumulation of large residual strains can exacerbate overall strain levels, potentially resulting in grain damage. This, in turn, poses risks to the safety, stability, and even the possibility of explosion of the engine. Hence, it is crucial to minimize residual strain of the grains of SRMs to ensure their reliability.

With the increasing loading ratio of SRMs, the residual strain in the grain from atmospheric pressure curing and cooling increases significantly, affecting the integrity of SRMs. Pressure curing molding technology can effectively reduce the residual strain in the grain. This technology involves applying pressure to the inside of the SRM before the cooling step. By elastically expanding the case through pressure application, the case shrinks during the cooling process due to the release of pressure. This elastic shrinkage deformation of the case offsets the thermal shrinkage deformation of the grain due to cooling, ultimately reducing residual strain in the grain. Scholars have carried out related research on pressure curing molding technology [4, 5], and the feasibility of this

technology has been verified through experiments [6]. Finite element methods have been used to study residual strain under pressure curing molding technology [7–9].

For SRMs, safety and integrity evaluation are crucial. While most analyses focus on the impact of temperature loading [10, 11], ignition pressurization [12–14], and aging effect [15–17] on the grain of SRMs, relatively few studies have been conducted on integrity analysis of SRMs based on residual strain, and an evaluation system has not yet been formed.

Hoop strain of the grain is a significant indicator for evaluating safety and integrity of SRMs. However, limited by measurement methods, obtaining grain strain data through tests is challenging. Theoretical calculations of strain changes under different load conditions can help with design and optimization of SRM structures.

This paper employs continuum mechanics to obtain basic solutions of the strain prediction function considering residual strain under pressure curing conditions. Viscoelastic material parameters of the grain are obtained through tests. The accuracy of assumptions and the theoretical model of the strain prediction function is verified by comparing with numerical results. Furthermore, the influence of curing pressure and hoop elastic modulus of the case is discussed based on strain prediction function. The results show that the pressure curing molding technology can effectively reduce the residual strain of the grain. There is an optimal curing pressure to minimize hoop strain reduction percentage, and for different case materials, a smaller hoop elastic modulus leads to smaller costs for achieving optimal curing pressure. This article provides guidance for the application of pressure curing molding technology.

The paper is structured as follows: Section 2 provides basic solutions of the strain prediction function. Viscoelastic material parameters of the grain are obtained through tests in Section 3. Section 4 verifies accuracy of assumptions and theoretical models of the basic solution by comparing with numerical results. Section 5 discusses influence of curing pressure and hoop elastic modulus of case based on strain prediction function. Finally, Section 6 summarizes main conclusions.

2. The Strain Prediction Function of Grain

The pressure curing molding technology is a useful method for reducing the residual strain of the grain, which can improve the safety and reliability of solid rocket motors (SRMs). This technology involves a two-stage manufacturing process, as shown in Figure 1.

The pressure curing molding technology consists of two stages in the manufacturing process of the grain. In the pressurization curing stage, the propellant is injected into the case in a liquid state. Pressure is applied inside the case, causing elastic expansion deformation, as shown in Figure 1(a). In the pressure relief cooling stage, pressure in the case is released and the propellant slurry solidifies into a solid propellant grain due to temperature drop. Here is a significant disparity in the thermal shrinkage between the grain and the case because of the large difference in thermal expansion coefficient between the grain and the case. After pressure relief, the case experiences shrinkage deformation,

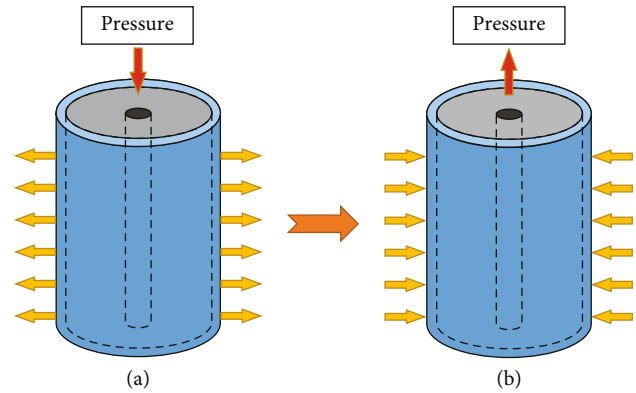

Figure 1: The process of the pressure curing molding technology: (a) pressurization stage; (b) cooling stage.

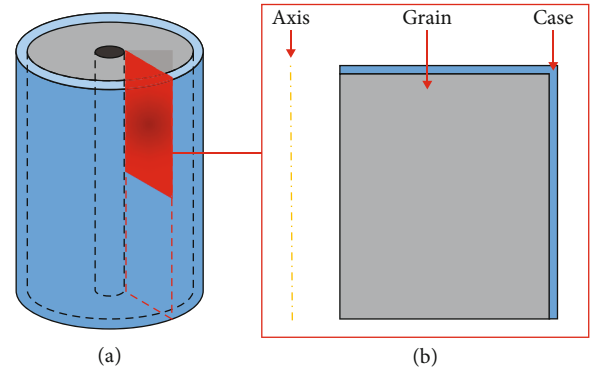

Figure 2: Structure diagram of theoretical model: (a) the three-dimensional method; (b) the 1/2 two-dimensional axisymmetric model.

equal to the expansion of the case during the pressurization curing stage, as shown in Figure 1(b). The elastic shrinkage deformation of the case can offset the thermal shrinkage deformation of the grain due to cooling. In this way, the residual strain of the grain can be reduced.

2.1. Theoretical Model of the Strain Prediction Function. The strain prediction function can quickly and efficiently obtain the strain of the grain without complicated numerical simulation. However, due to the complexity of the SRM structure, simplifications are necessary. In this paper, we make the following assumptions:

(1) The SRM model is simplified as cylinders, including a thin-walled cylinder (case) and a thick-walled cylinder (grain), with the shape of the grain ignored

(2) Only the initial and final states of the grain are considered, so the grain is considered as a linear elastic material for calculation

(3) The influence of the thermal insulation layer is ignored due to its small thickness and low modulus

For convenience, the model is simplified to a 1/2 two-dimensional axisymmetric model, as shown in Figure 2.

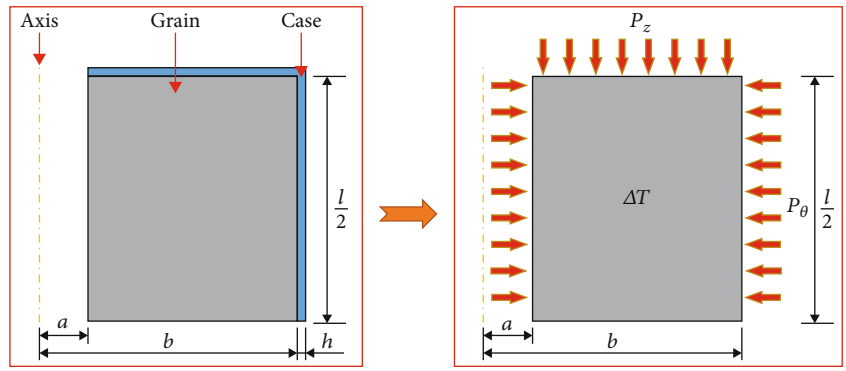

Figure 3: The mechanical analysis model of the thick-walled cylinder.

2.2. Basic Solution of Thick-Walled Cylinder. During the life cycle of the SRM, the grain is subjected to temperature loads and pressure loads. If the inner surface of the grain is subjected to pressure, a compressive stress will be generated between the grain and the case, which is equivalent to the outer surface of the grain also being subjected to pressure. Assume that the pressure on the inner cylindrical surface of the grain is P_1, the pressure on the outer cylindrical surface is P_θ, and the pressure on the axial surface is P_z, as shown in Figure 3. Therefore, the strain analysis of the grain can be transformed into the problem of thick-walled cylinder.

In polar coordinates, according to the Lamé equation, the stress of a thick-walled cylinder under pressure is

$$\begin{cases} \sigma_\theta^g = B + \dfrac{A}{r^2}, \\ \sigma_r^g = B - \dfrac{A}{r^2}, \\ \sigma_z^g = -P_z, \end{cases} \quad \begin{cases} A = \dfrac{(P_\theta - P_1)a^2b^2}{b^2 - a^2}, \\ B = \dfrac{a^2P_1 - b^2P_\theta}{b^2 - a^2}, \end{cases} \tag{1}$$

where σ_θ^g, σ_r^g, and σ_z^g are the hoop stress, radial stress, and axial stress of the case caused by interfacial forces, respectively, a is the radius of the inner cylindrical surface of the grain, and b is the radius of outer cylindrical surface.

Based on the generalized Hooke's law, the strain of the grain can be obtained using Equation (1):

$$\begin{cases} \varepsilon_\theta^g(r) = \dfrac{1}{E_g}\left[\left(1-\mu_g\right)B - \left(1+\mu_g\right)\dfrac{A}{r^2}\right] + \dfrac{\mu_g P_z}{E_g}, \\ \varepsilon_r^g(r) = \dfrac{1}{E_g}\left[\left(1-\mu_g\right)B + \left(1+\mu_g\right)\dfrac{A}{r^2}\right] + \dfrac{\mu_g P_z}{E_g}, \\ \varepsilon_z^g(r) = -\dfrac{2}{E_g}\mu_g B - \dfrac{P_z}{E_g}, \end{cases} \tag{2}$$

where ε_θ^g, ε_r^g, and ε_z^g are the hoop strain, radial strain, and axial strain of the grain caused by pressure loads, respectively, E_g is the elastic modulus of the grain, and μ_g is its Poisson's ratio. If the thick-walled cylinder is subjected to temperature loads, then it needs to consider a temperature term in the strain:

$$\begin{cases} \varepsilon_\theta^g(r) = \dfrac{1}{E_g}\left[\left(1-\mu_g\right)B - \left(1+\mu_g\right)\dfrac{A}{r^2}\right] + \dfrac{\mu_g P_z}{E_g} + \alpha_g \Delta T, \\ \varepsilon_r^g(\mathrm{r}) = \dfrac{1}{E_g}\left[\left(1-\mu_g\right)B + \left(1+\mu_g\right)\dfrac{A}{r^2}\right] + \dfrac{\mu_g P_z}{E_g} + \alpha_g \Delta T, \\ \varepsilon_z^g(r) = -\dfrac{2}{E_g}\mu_g B - \dfrac{P_z}{E_g} + \alpha_g \Delta T, \end{cases} \tag{3}$$

where α_g is the thermal expansion coefficient of the grain and ΔT is the temperature difference.

The displacement of the grain can be described as

$$\begin{cases} u_\theta^g(r) = \dfrac{1}{E_g}\left[\left(1-\mu_g\right)Br - \left(1+\mu_g\right)\dfrac{A}{r}\right] + \dfrac{r\mu_g P_z}{E_g} + r\alpha_g \Delta T, \\ u_z^g(z) = -\dfrac{2z}{E_g}\mu_g B - \dfrac{zP_z}{E_g} + z\alpha_g \Delta T. \end{cases} \tag{4}$$

The strain needs to be solved based on the boundary conditions of the thick-walled cylinder. At different stages of SRM, different loads act on the grain; therefore, its boundary conditions also differ. Next, the boundary conditions under different loads need to be investigated.

2.2.1. Temperature Load Condition. In SRM production processes, residual strain appears in the grain under temperature load. The grain and case of a solid rocket motor can be approximated as continuous, fully filled space media. Therefore, at the interface between the grain-case, the stress field and displacement field of the grain and case should be continuous. Thus, the boundary conditions of the model at this stage can be expressed as

$$\begin{cases} \sigma_r^g(a) = 0, \\ \sigma_r^g(b) = P_\theta, \\ \sigma_z^g\left(\dfrac{l}{2}\right) = P_z, \end{cases} \quad \begin{cases} u_r^g(b) = u_b^c, \\ u_z^g\left(\dfrac{l}{2}\right) = u_{l/2}^c. \end{cases} \tag{5}$$

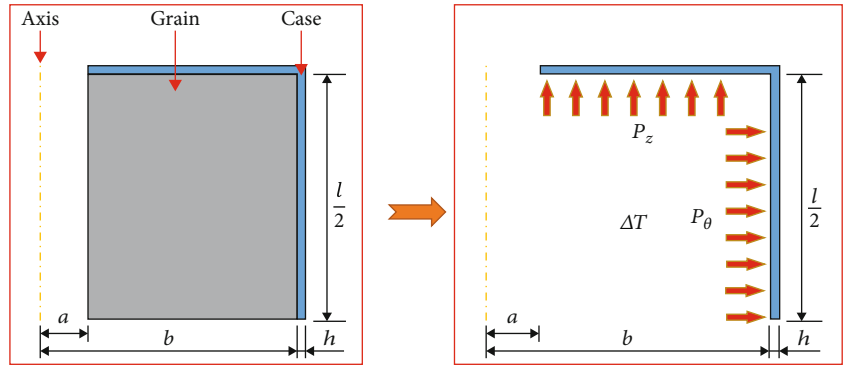

Figure 4: The mechanical analysis model of the thin-walled cylinder.

However, P_θ and P_z are unknown quantities. Therefore, in order to obtain the basic solution of strain, it is necessary to analyze the thin-walled cylinder with a mechanical analysis model shown in Figure 4.

Based on pressure curing molding technology, displacement of the thin-walled cylinder consists of three parts: $u_b^{c,T}$ or $u_{l/2}^{c,T}$ caused by temperature difference, $u_b^{c,P}$ or $u_{l/2}^{c,P}$ caused by pressure at grain-case interface, and $u_b^{c,\text{curing}}$ or $u_{l/2}^{c,\text{curing}}$ caused by the pressure release in pressure relief stage. The displacement of the thin-walled cylinder u_b^c or $u_{l/2}^c$ can be expressed as

$$\begin{cases} u_b^c = u_b^{c,T} + u_b^{c,P} + u_b^{c,\text{curing}}, \\ u_{l/2}^c = u_{l/2}^{c,T} + u_{l/2}^{c,P} + u_{l/2}^{c,\text{curing}}. \end{cases} \tag{6}$$

In particular, for orthotropic materials, Equation (6) can be expressed as

$$\begin{cases} u_b^{c,T} = b\alpha_c \Delta T, \\ u_{l/2}^{c,T} = \dfrac{l}{2}\alpha_c \Delta T, \end{cases} \tag{7}$$

$$\begin{cases} u_b^{c,P} = b\dfrac{b}{E_\theta h}P_\theta - b\dfrac{\mu_{\theta z}\left(b^2 - a^2\right)}{2hE_\theta b}P_z, \\ u_{l/2}^{c,P} = -\dfrac{l}{2}\dfrac{\mu_{z\theta} b}{E_z h}P_\theta + \dfrac{l}{2}\dfrac{b^2 - a^2}{2hE_z \mathrm{b}}P_z, \end{cases} \tag{8}$$

$$\begin{cases} u_b^{c,\text{curing}} = -b\dfrac{(2-\mu_{\theta z})b^2 + \mu_{\theta z}a^2}{2E_\theta hb}P^{\text{cur}}, \\ u_{l/2}^{c,\text{curing}} = -\dfrac{l}{2}\dfrac{(1-2\mu_{z\theta})b^2 - a^2}{2E_z hb}P^{\text{cur}}, \end{cases} \tag{9}$$

where E_θ and E_z are hoop and axial elastic moduli of the case, respectively; $\mu_{\theta z}$ and $\mu_{z\theta}$ are Poisson's ratios of the case, respectively; and P^{cur} is pressure of pressure curing molding technology.

P_θ and P_z can be obtained by solving Equation (5), and then, Equation (3) can be used to calculate residual strain for the thick-walled cylinder. This equation is also applicable to casting molding technology, only need to set $P^{\text{cur}} = 0$.

2.2.2. Pressure Load Condition. During the working process of SRM, ignition pressure P_θ acts on inner surface of the grain for an extremely short time (0.1 s). Therefore, it is considered that temperature does not change in this stage. Thus, the boundary conditions of the model are express as

$$\begin{cases} \sigma_r^g(a) = P_1, \\ \sigma_r^g(b) = P_\theta, \\ \sigma_z^g(l/2) = P_Z, \end{cases} \quad \begin{cases} u_r^g(b) = u_b^c, \\ u_z^g(l/2) = u_{l/2}^c. \end{cases} \tag{10}$$

The displacement of the thin-walled cylinder u_b^c or $u_{l/2}^c$ in working process can be expressed as

$$\begin{cases} u_b^c = u_b^{c,P} = b\dfrac{b}{E_\theta h}P_\theta - b\dfrac{\mu_{\theta z}\left(b^2 - a^2\right)}{2hE_\theta b}P_z, \\ u_{l/2}^c = u_{l/2}^{c,P} = -\dfrac{l}{2}\dfrac{\mu_{z\theta} b}{E_z h}P_\theta + \dfrac{l}{2}\dfrac{b^2 - a^2}{2hE_z b}P_z. \end{cases} \tag{11}$$

Similarly, P_θ and P_z can be obtained by solving Equation (10). Because residual strain is generated in the production process of grain, it should be added to model as initial condition in working process of grain. Then, Equation (12) can be used to obtain strain for grain:

$$\begin{cases} \varepsilon_\theta^g(r) = \dfrac{1}{E_g}\left[\left(1-\mu_g\right)B - \left(1+\mu_g\right)\dfrac{A}{r^2}\right] + \dfrac{\mu_g q_z}{E_g} + \varepsilon_\theta^R(r), \\ \varepsilon_r^g(r) = \dfrac{1}{E_g}\left[\left(1-\mu_g\right)B + \left(1+\mu_g\right)\dfrac{A}{r^2}\right] + \dfrac{\mu_g q_z}{E_g} + \varepsilon_r^R(r), \\ \varepsilon_z^g(r) = -\dfrac{1}{E_g}2\mu_g B - \dfrac{q_z}{E_g} + \varepsilon_z^R(r), \end{cases} \tag{12}$$

where ε_θ^R, ε_r^R, and ε_z^R are the residual strains obtained in Section 2.2.1.

3. Mechanical Test of Grain

3.1. Stress Relaxation Test. Grain exhibits classic viscoelastic response to loading and is subject to property degradation

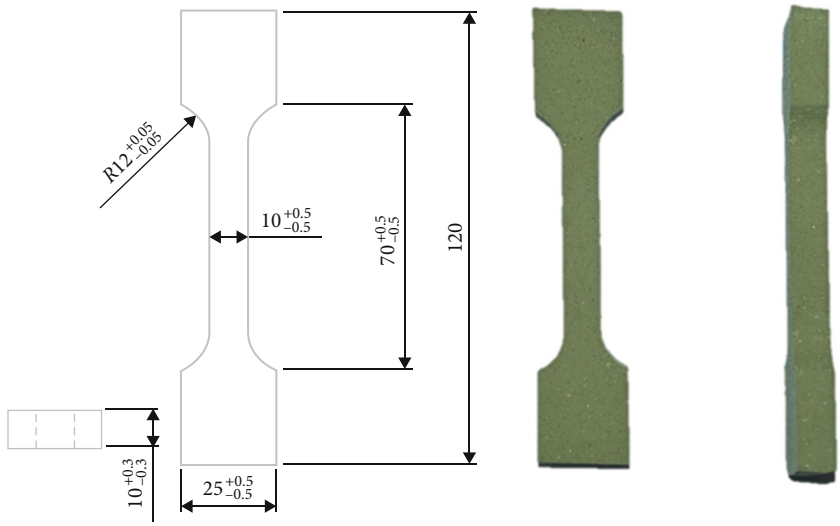

Figure 5: Specimen and its size.

over time. Therefore, the grain is generally regarded as a viscoelastic material during analysis. The integral-type constitutive equation for viscoelastic materials is shown in

$$\sigma = \int_0^t E(t-\tau)\frac{\partial \varepsilon}{\partial \tau}d\tau, \tag{13}$$

where $E(t)$ is the relaxation modulus, t is the time, and the time argument τ is specified as the variable of integration.

For viscoelastic materials, the phenomenon of stress decreasing with time when strain $\varepsilon(t) = \varepsilon_0 H(t)$ is applied is called stress relaxation. Where $H(t)$ is Heaviside function defined as:

$$H(t) = \begin{cases} 0, & t < 0, \\ 1, & t > 0. \end{cases} \tag{14}$$

Relaxation test is the most common approach to determine relaxation properties of the materials. To determine the relaxation modulus, a relaxation test was conducted according to the aerospace industry standard of PRC, QJ 2487-93. The test specimen used for the relaxation test is illustrated in Figure 5. The specimen was initially stretched at a tensile rate of 100 mm/min, and when the strain of the specimen reached 5%, it was held constant for 1000 s.

The relaxation modulus was calculated using Equation (15), and the test was repeated five times to obtain the average relaxation modulus.

$$E(t) = \frac{F(t)(1+\varepsilon_0)}{A_0\varepsilon_0}, \tag{15}$$

where $F(t)$ is the relaxation force at the corresponding moment, ε_0 is the initial strain value, and A_0 is the initial cross-sectional area of specimen. The relaxation modulus can be fitted using the Prony series, as shown in Equation (16). The test curve and fitted curve of the relaxation modulus are shown in Figure 6.

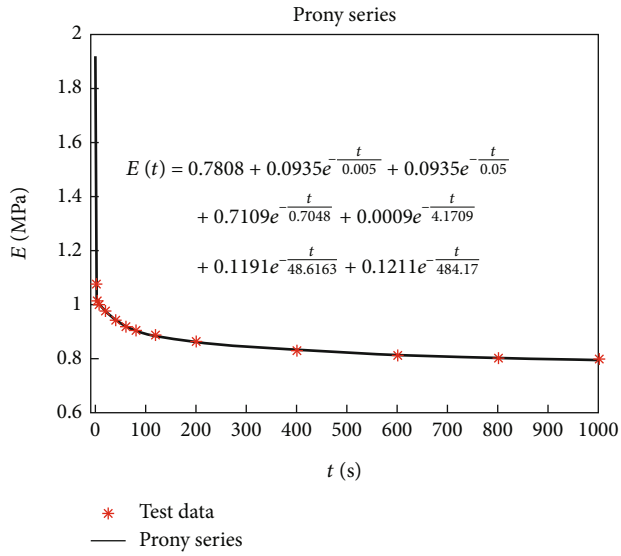

Figure 6: Test curve and Prony series fitting curve of the relaxation modulus.

$$E(t) = E_\infty + \sum_{i=1}^{n} E_i e^{-t/\tau_i}, \tag{16}$$

where E_i and τ_i represent the parameters of the Prony series.

The relaxation modulus at $t = 0$ is referred to as the initial modulus ($E_0 = 1.9198$ MPa), while at $t = 1000$, it is known as the equilibrium modulus ($E_\infty = 0.7808$ MPa).

3.2. Ground Test. The accuracy of the strain prediction function needs to be verified by measuring the strain of the grain in the ground test; however, it is difficult to measure the strain of the grain in the test, so the hoop strain on the outer surface of the SRM case is measured to indirectly provide support for verifying the accuracy of the strain prediction function.

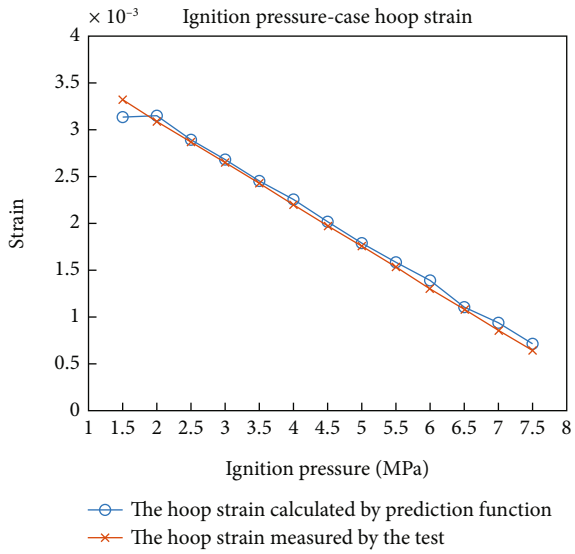

Figure 7: Comparison of the measured hoop strain of the case in the ground test with the predicted hoop strain.

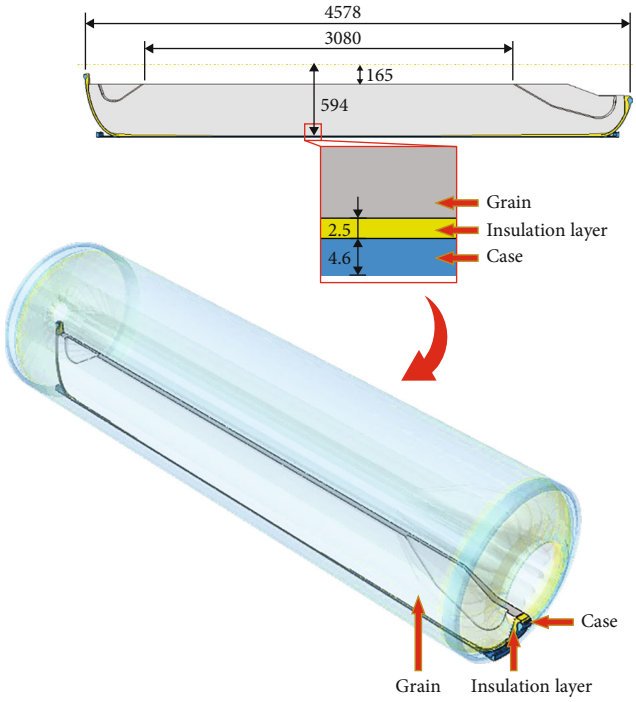

Figure 8: Finite element model of SRM.

A cylindrical SRM was used for ground test. The radius of the SRM case is 375 mm, the radius of the inner surface of the grain is 100 mm, and the thickness of the case is 3.5 mm. The Poisson ratio of the grain is 0.4999, and the elastic modulus of the grain is 0.7808 MPa during the cooling process and 1.9198 MPa during the ignition process. The Poisson ratio of the case is 0.285, and the elastic modulus is 206 GPa. The SRMs used for ground test were produced under the cast molding technology. During the ignition process, a comparison of the hoop strain of the case measured by the ground test with the predicted strain is shown in Figure 7. It can be figured out that the strain measured by the ground test is in good agreement with the calculation result by prediction function.

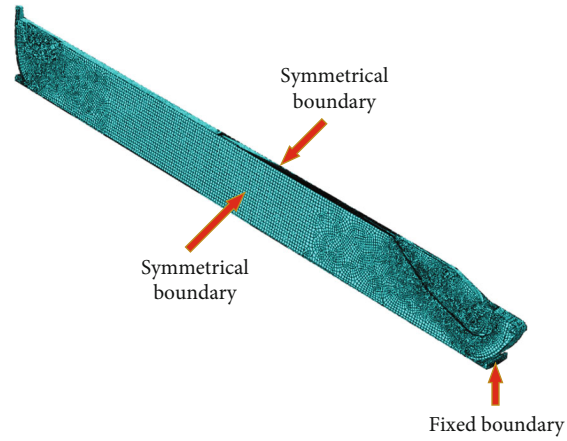

Figure 9: Elements and boundary conditions of the model.

Table 1: Viscoelastic material parameters.

τ_1 (s)	τ_2 (s)	τ_3 (s)	τ_4 (s)	τ_5 (s)	τ_6 (s)
0.005	0.05	0.7048	4.1709	48.617	484.17
E_1 (MPa)	E_2 (MPa)	E_3 (MPa)	E_4 (MPa)	E_5 (MPa)	E_6 (MPa)
0.0935	0.0935	0.7109	0.0009	0.1191	0.1211
E_∞ (MPa)	μ	α (°C^{-1})			
0.7808	0.4995	1×10^{-4}			

Table 2: Orthotropic material parameters.

E_r (GPa)	E_θ (GPa)	E_z (GPa)	$G_{r\theta}$ (GPa)	$G_{\theta z}$ (GPa)
6.7	77	58.1	5.26	19.1
G_{rz} (GPa)	$\mu_{r\theta}$	$\mu_{\theta z}$	μ_{rz}	α (°C^{-1})
5.26	0.23	0.192	0.1	3×10^{-7}

4. Numerical Validation

In Section 2, a strain prediction function of the grain under pressure curing molding technology is obtained based on a series of assumptions and an ideal cylinder model. The proposed function ignores the effect of the real structure of the grain. Therefore, to verify the predictive capability of the proposed function, a numerical simulation analysis based on real grain structure was carried out using the finite element method.

4.1. Model and Material Parameters. This paper modeled the case, insulation layer, and grain structure of the SRM separately. The dimensions of the SRM are shown in Figure 8, where the total length of the model is 4578 mm and the length of the cylindrical part is 3080 mm. For the cylindrical part, the radius of the case is 594 mm, the radius of the inner surface of the grain is 165 mm, the thickness of the insulation layer is 2.5 mm, and the thickness of the case is 4.6 mm. Due to the symmetry of the

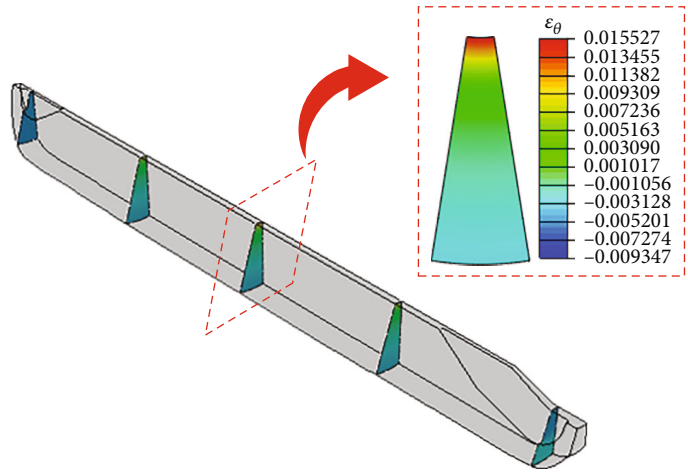

Figure 10: Hoop residual strain at different positions of grain.

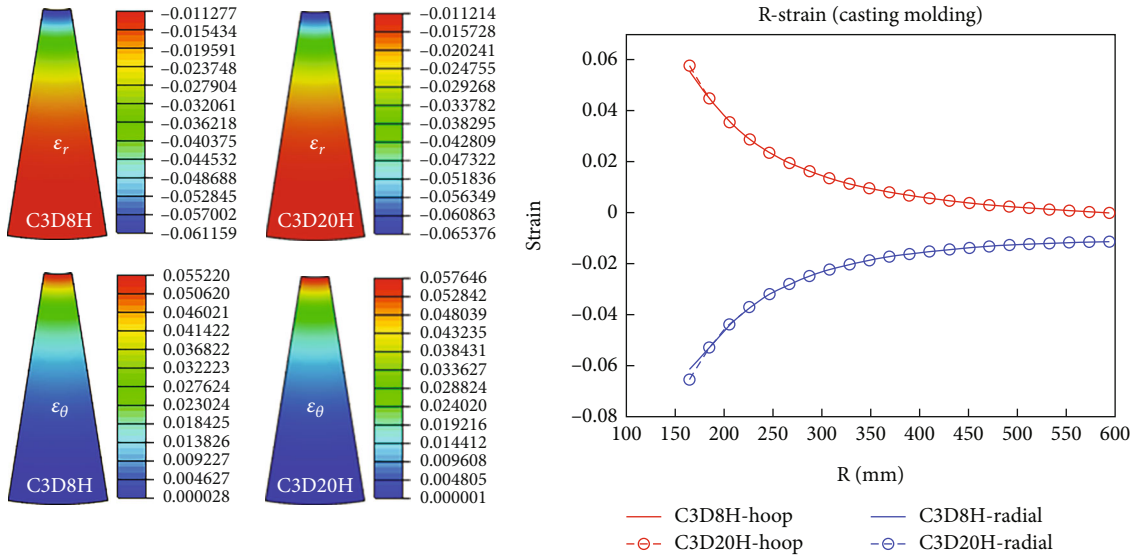

Figure 11: Comparison of hoop residual strain and radial residual strain for numerical solutions of C3D8H and C3D20H elements: (a) strain field in the middle of the simulation model; (b) strain distribution in the radial direction.

SRM structure, a 1/20 model is used for simulation analysis to save computational resources without losing effectiveness, as shown in Figure 8.

Figure 9 shows the grid division and boundary conditions of the model. The total number of elements in the model was 296254, including 275212 elements for the grain, 8442 elements for the insulation layer, and 12600 elements for the case. The end face of the shell was applied with fixed boundary condition, while the side faces of the model were applied with symmetry boundary conditions. Symmetry boundary conditions were set by fixing the hoop translations, normal rotations, and axial rotations of the side faces in the cylindrical coordinate system.

4.2. Cooling Process Based on Pressure Curing Molding Technology. This paper presents an improved two-step analysis method, based on reference [7], for simulating the manufacturing process of grain using pressure curing molding technology in the SRM. The process involves pressurization curing and pressure relief cooling stages.

During the pressurization process, pressure is applied on the inner surface of the case, while the inner hole of the model is fixed. The model expands under pressure, approximating the process of model volume expansion caused by pressure curing. The modulus and Poisson's ratio of propellant slurry are 0.001 MPa and 0.495, respectively.

In the cooling process, the model after the first step of deformation is extracted as the analysis model. The stress results of the case in the first step are extracted as the prestrain in the second step, which simulates the shrinkage process after pressure release. At this step, SRM decreases from production temperature (58°C) to room temperature (20°C). The propellant slurry transforms into solid viscoelastic

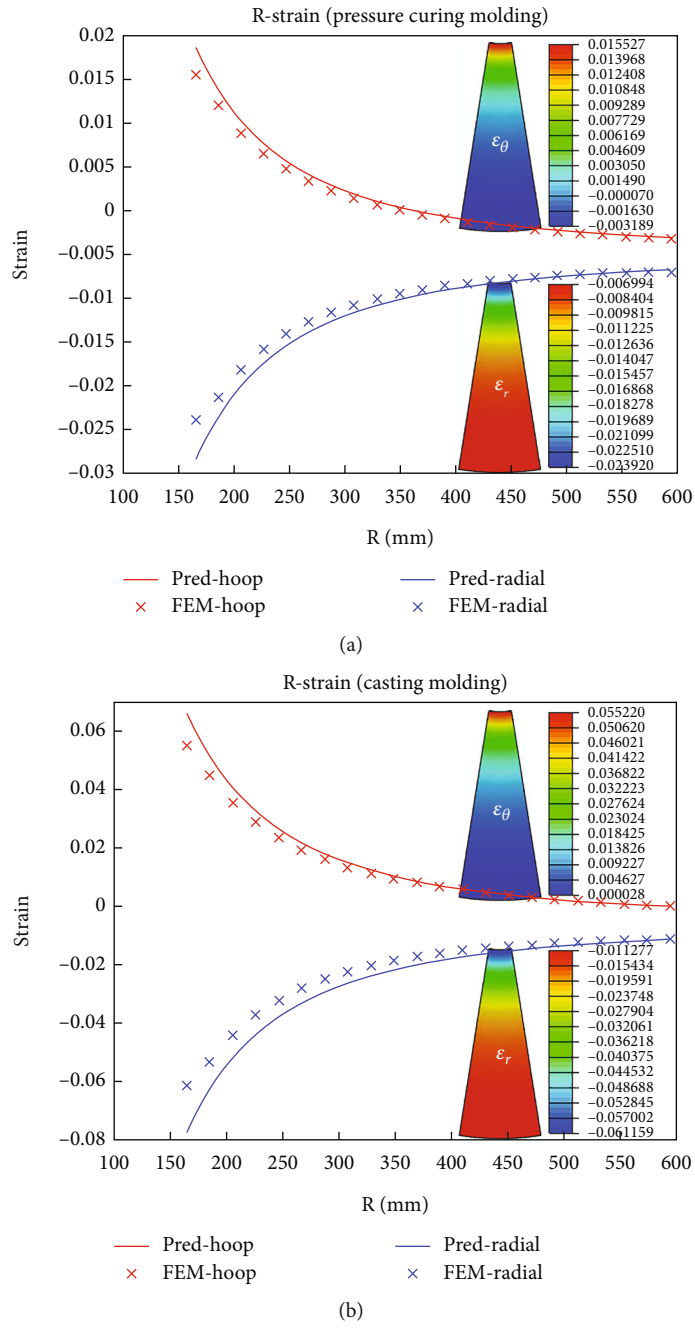

Figure 12: Comparison of hoop residual strain and radial residual strain between strain prediction function and numerical results: (a) pressure curing molding technology; (b) casting molding technology.

grain. The viscoelastic parameters are given by the tests in Section 3 and can be found in Table 1.

Throughout the entire process, both the case and insulation layer maintain their original material properties. The material properties of the case can be found in Table 2. The insulation layer is regarded as a linear elastic material with a modulus of 1 MPa, a Poisson ratio of 0.4995, and a linear expansion coefficient of $1.3 \times 10^{-4}°C^{-1}$.

The long-time ($>10^4$ s) temperature load (-38°C) causes residual strain in the grain. The numerical results of hoop residual strain at different positions of grain are shown in Figure 10. The strain is most pronounced at the middle position of the grain, as it is less affected by the SRM structure and closer to the theoretical model of the strain prediction function discussed in Section 2. Because the residual strain is highest in the middle position, this is also where the grain is most likely to be damaged. Consequently, in subsequent analysis, we verify the accuracy of the strain prediction function by comparing the strain in the middle of the simulation model with predicted strain.

The hybrid element C3D8H in Abaqus is used for the grain and insulation layer to avoid the self-locking problem

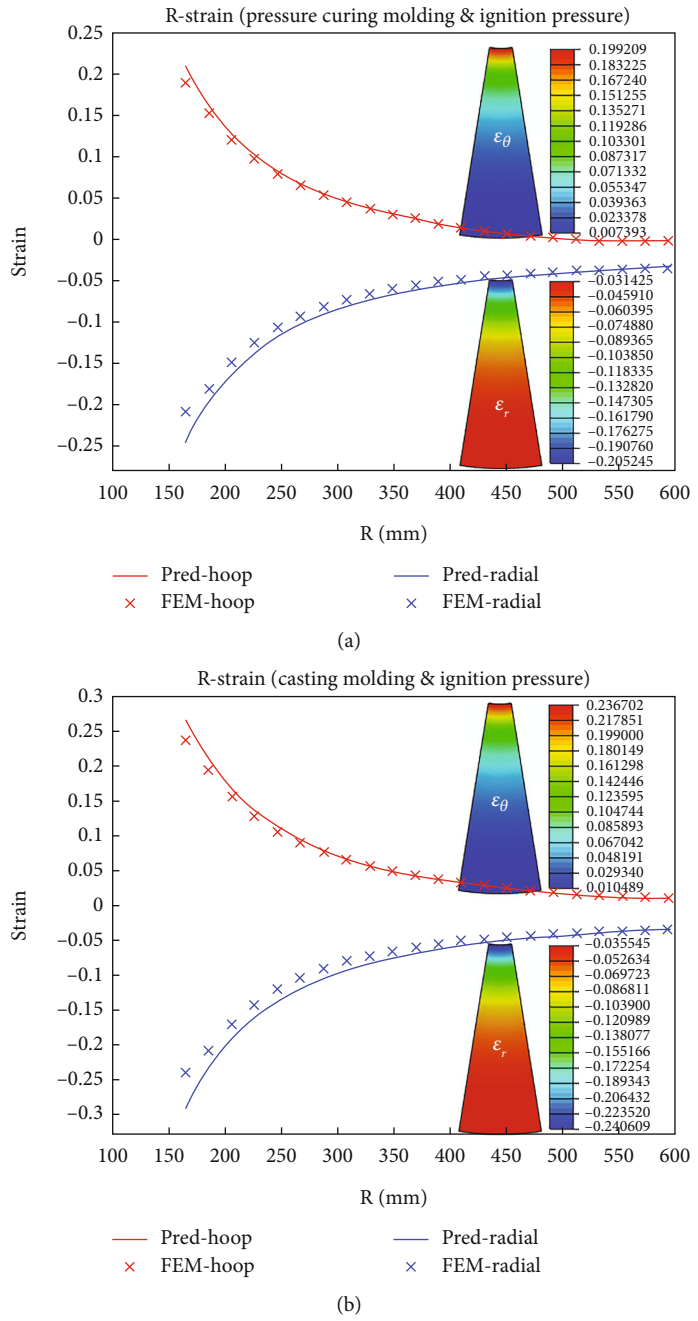

Figure 13: Comparison of hoop strain and radial strain between strain prediction function and numerical results: (a) pressure curing molding technology; (b) casting molding technology.

of the high Poisson's ratio. In order to verify the difference between the two hybrid elements, C3D8H and C3D20H, this paper first numerically simulates the cooling process under casting molding technology. C3D8H and C3D20H are used for the grain as well as the insulation layer, respectively, and C3D8 is always used for the case. Figure 11(a) shows the strain field in the hoop as well as radial direction at the center of the model, and Figure 11(b) shows the strain variation along the radial direction of the strain field. The comparison shows that the difference between the strains of C3D20H and C3D8H is greater on the inner surface of the grain than on the outer surface of the grain, but all the differences are within tolerance. However, the numerical analysis using C3D20H requires much more computer performance and computational time than using C3D8H. Therefore, combining the accuracy of the numerical analysis and the computational cost, C3D8H is used for the grains and the insulation layer and C3D8 is used for the case in all the numerical analyses below.

The comparison between predicted strain function and simulation model under different casting conditions is shown in Figure 12. The results indicate that coincidence between

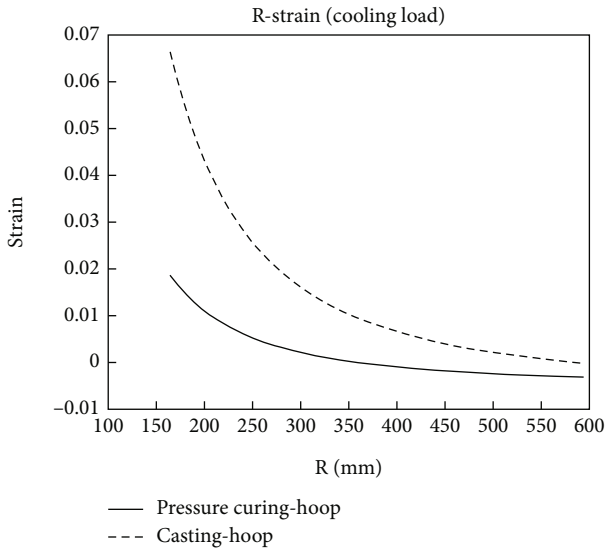

Figure 14: The hoop residual strain at the inner surface under the casting molding technology and the pressure curing molding technology.

numerical results and predicted values is high for radial and axial directions. The largest error is observed at inner hole of grain, which is influenced by stress release boot at both ends of SRM. Overall, strain prediction function can predict residual strain at most critical position of grain during cooling process, and thus, assumptions and theoretical model of strain prediction function in Section 2 are deemed acceptable.

4.3. Ignition Process Based on Residual Strain. During working process of SRM, inner hole of grain was subjected to a pressure (6.28 MPa) lasting for 0.1 s, resulting in deformation of grain. In this process, influence of residual strain of grain cannot be ignored. Therefore, residual strain of grain was considered as initial state of model under ignition pressure load. The results are shown in Figure 13. Although absolute value of numerical results is slightly lower than predicted value due to stress release boot of grain, coincidence degree of two is within tolerance range. Hence, it can be concluded that strain prediction function can predict strain at most critical position of grain in working process, which also validates rationality of assumptions and theoretical model of strain prediction function.

5. Discussion

Accurately predicting the strain in the grain under pressure curing conditions is crucial for the design of the SRM [18]. Figure 14 shows that under pressure curing molding technology, for a specific SRM size, a curing pressure of 2 MPa can significantly reduce the residual strain in the hoop direction due to the temperature decrease during the manufacturing process of the grain, which can reduce the total strain of the grain during storage and working processes, and improve the safety and stability of the SRM.

Overall, the hoop residual strain of the grain is maximum at the inner surface. The value gradually decreases

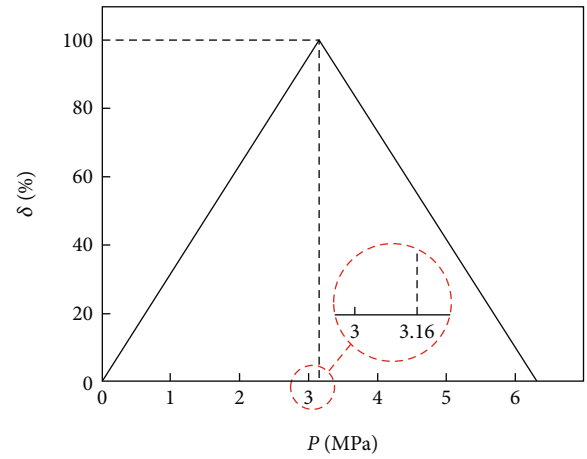

Figure 15: The relationship between the hoop strain reduction δ and curing pressure P.

along the radial direction and tends to be constant when it is close to the outer surface of the grain. Compared with the casting molding technology, the hoop residual strain was reduced from the inner surface to the outer surface of the grain under the pressure curing molding technology, with the greatest reduction at the inner surface. Therefore, the reduction of hoop residual strain at the inner surface under different casting conditions is used to numerically characterize the effect of pressure curing on residual strain, as shown in

$$\delta = \frac{\left|\varepsilon_\theta^c\right| - \left|\varepsilon_\theta^p\right|}{\left|\varepsilon_\theta^c\right|} \times 100, \tag{17}$$

where δ is the hoop strain reduction, ε_θ^c is the hoop strain on the inner surface of the grain under the casting molding technology, and ε_θ^p is the hoop strain on the inner surface of the grain under the pressure curing molding technology.

For pressure curing molding technology, the greater the hoop strain reduction δ, the smaller the hoop residual strain. Figure 15 shows the relationship between the hoop strain reduction δ and curing pressure P. The hoop strain reduction δ under pressure curing molding technology initially increases and then decreases with the increase of curing pressure P. When the curing pressure is 3.16 MPa, δ is 100%, which means that the hoop strain on the inner surface of the grain becomes 0. However, when the pressure exceeds 3.16 MPa, the elastic deformation of the case becomes too large, causing the hoop strain on the inner surface of the grain to change from tensile strain to compressive strain and gradually increases. This is why the hoop strain reduction percentage decreases. Therefore, there is an optimal value of curing pressure that can make the efficiency of pressure curing molding technology optimal.

The optimum curing pressure is a constant number for a given SRM size. Ideally, the optimum curing pressure can be used to reduce the residual strain of the grain to 0. In practical engineering applications, the curing pressure may not reach the optimal value due to equipment and cost

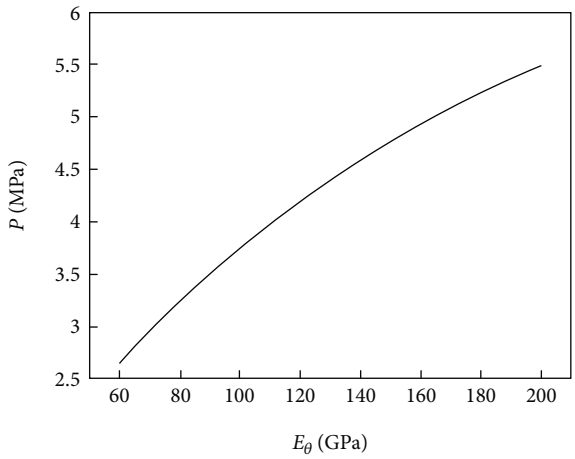

Figure 16: The relationship between the optimal curing pressure P and the hoop elastic modulus of case E_θ.

constraints, but it can be kept as close to the optimum value as possible to minimize residual strain caused during the cooling process of the grain.

Moreover, the elastic modulus of the case also affects the efficiency of pressure curing molding technology. The hoop elastic modulus of the case has a significant impact on pressure curing for orthotropic materials [18]. Therefore, the relationship between optimal curing pressure and hoop elastic modulus of the case was studied, as shown in Figure 16. For the same grain material, the larger the hoop elastic modulus of the case, the greater the optimal curing pressure. This means that materials with lower hoop elastic modulus are more appropriate as a case material under pressure curing molding technology since they require lower costs to achieve optimal curing pressure.

For pressure curing molding technology, the smaller the hoop modulus, the easier it is to achieve the optimum curing pressure for a given size of case. However, the case also needs sufficient strength to protect the grain. Therefore, it is necessary to find a suitable solution for the case material, so that both the hoop modulus and the optimal curing pressure are within tolerable limits. Compared with metal materials, composite materials are more suitable as case materials. This is because it saves costs by reducing both the weight of the case and the optimum curing pressure while providing sufficient strength.

6. Conclusion

In this paper, a strain prediction function for the grain under pressure curing molding technology was derived. The assumptions and theoretical model of the strain prediction function were verified using the finite element method. And the efficiency of pressure curing molding technology and its influencing factors on optimal curing pressure were discussed. The following conclusions were drawn:

(1) The strain prediction function of the grain was established based on continuum mechanics, which effectively predicted the strain of the grain during cooling and working processes. The strain under pressure curing molding technology was decomposed into thermal strain and mechanical strain according to the superposition principle. The basic solution was obtained by solving displacement continuity between grain and the case at the interface

(2) The pressure curing molding technology was simulated using a modified two-step analysis method. By comparing the numerical results with the predicted values, the rationality of the assumptions and theoretical model was verified. The strain prediction function accurately predicted the strain distribution at the most critical position in grain

(3) Pressure curing molding technology can effectively reduce the residual strain of the grain. An optimal value of curing pressure exists, which makes the efficiency of pressure curing molding technology optimal. For materials with lower hoop elastic modulus, such as composites, the optimal efficiency of pressure curing molding technology can be achieved with lower curing pressure

Data Availability

As most of the data in this manuscript were related to trade secrets, I cannot provide them completely. In the future, if necessary, I can share some data with reviewers or readers.

Conflicts of Interest

The authors declare that there is no conflict of interest regarding the publication of this paper.

Acknowledgments

This work was supported by the Application Innovation Plan Project of China Aerospace Science and Technology Group, the Basic Research Project (No. 514010304-302-2), and the National Natural Science Foundation of China (No. 11772245).

References

[1] W. M. Adel and G. Z. Liang, "Study of cooldown thermal loading effect on the bore deformation of viscoelastic solid propellant grain," in *Proc. 53rd AIAA/SAE/ASEE Joint Propulsion Conference*, vol. 4692, Atlanta, GA, 2017.

[2] Z. Cui, H. Li, Z. Shen, and H. Cui, "A viscoelastic constitutive model of propellant with pressure cure," *Propellants, Explosives, Pyrotechnics*, vol. 46, no. 7, pp. 1036–1048, 2021.

[3] H. T. Chu and J. H. Chou, "Poisson ratio effect on stress behavior of propellant grains under ignition loading," *Journal of Propulsion and Power*, vol. 27, no. 3, pp. 662–667, 2011.

[4] D. A. Hunt, "Computing pressure cure viscoelastic effects in solid propellants," *Journal of Spacecraft and Rockets*, vol. 9, no. 12, pp. 937-938, 1972.

[5] R. A. Ellis, R. N. Hammond, and P. Donguy, "Advanced space motor demonstration," *Journal of Spacecraft and Rockets*, vol. 19, no. 1, pp. 60–65, 1982.

[6] K. J. Arai, "Research on pressure cure of solid rocket motor," *Industry Powder*, vol. 43, no. 6, pp. 360–367, 1982.

[7] L. Zong, C. Du, S. Lu, D. Yao, J. Gao, and B. Sha, "Simulation on pressure curing of solid rocket motor grain," *Journal of Solid Rocket Technology*, vol. 38, no. 5, pp. 653–656, 2015.

[8] Z. Liu, E. Quan, Y. Chu, R. Jin, P. Ren, and L. Chen, "Theoretical and simulation research on pressure curing of solid rocket motor," *Journal of Solid Rocket Technology*, vol. 42, no. 5, pp. 576–579, 2019.

[9] Z. Cui, H. Li, Z. Shen, and H. Cui, "Analysis of load optimization in solid rocket motor propellant grain with pressure cure," *International Journal of Aerospace Engineering*, vol. 2021, Article ID 5026878, 11 pages, 2021.

[10] S. W. Chyuan, "Numerical study of solid propellant grains subjected to unsteady state thermal loading," *International Journal of Computer Applications in Technology*, vol. 24, no. 2, pp. 98–109, 2005.

[11] T. Li, B. Lu, and Z. An, "Response analysis of HTPB propellant under extreme high temperature conditions," in , Article ID 042057*Proc. The third Energy Technologies and Power Engineering*, vol. 769, Changsha, China, 2021.

[12] S. W. Chyuan, "Studies of Poisson's ratio variation for solid propellant grains under ignition pressure loading," *International Journal of Pressure Vessels and Piping*, vol. 80, no. 12, pp. 871–877, 2003.

[13] H. Chu and J. Chou, "Effect of cooling load on the safety factor of propellant grains," *Journal of Propulsion and Power*, vol. 29, no. 1, pp. 27–33, 2013.

[14] J. Wang, F. Bao, and H. Cui, "Structural analysis of solid rocket motor with effects of viscoelastic Poisson's ratio," in , Article ID 012020*Proc. 2022 International Conference on Materials Engineering and Applied Mechanics*, vol. 2285, Changsha, China, 2022.

[15] Ş. Özüpek, "Computational procedure for the life assessment of solid rocket motors," *Journal of Spacecraft and Rockets*, vol. 47, no. 4, pp. 639–648, 2010.

[16] H. C. Yıldırım and Ş. Özüpek, "Structural assessment of a solid propellant rocket motor: effects of aging and damage," *Aerospace Science and Technology*, vol. 15, no. 8, pp. 635–641, 2011.

[17] B. Deng, G. Tang, and Z. Shen, "Structural analysis of solid rocket motor grain with aging and damage effects," *Journal of Spacecraft and Rockets*, vol. 52, no. 2, pp. 331–339, 2015.

[18] C. Wang and W. Tian, "The influence factors of grain integrity under the internal pressure condition in SRM," *International Journal of Aerospace Engineering*, vol. 2021, Article ID 5521455, 8 pages, 2021.